Alzheimer's & Dementia: Diagnosis, Assessment & Disease Monitoring 11 (2019) 538-549

Working Group Summaries for European Joint Programming For Neurodegenerative Research (JPND)

European Ultrahigh-Field Imaging Network for Neurodegenerative Diseases (EUFIND)

Emrah Düzel[a,b,c,d,*], Julio Acosta-Cabronero[b,e], David Berron[b,f], Geert Jan Biessels[g], Isabella Björkman-Burtscher[f,h], Michel Bottlaender[i], Richard Bowtell[j], Mark v Buchem[k], Arturo Cardenas-Blanco[a,b], Fawzi Boumezbeur[i], Dennis Chan[l], Stuart Clare[m], Mauro Costagli[n,o], Ludovic de Rochefort[p], Ariane Fillmer[q], Penny Gowland[j], Oskar Hansson[f,r], Jeroen Hendrikse[g], Oliver Kraff[s], Mark E. Ladd[t,u], Itamar Ronen[k], Esben Petersen[v], James B. Rowe[l], Hartwig Siebner[v,w], Tony Stoecker[x], Sina Straub[t], Michela Tosetti[n,o], Kamil Uludag[y,z], Alexandre Vignaud[i], Jaco Zwanenburg[g], Oliver Speck[b,d,aa,bb]

[a]*Institute of Cognitive Neurology and Dementia Research, Otto-von-Guericke University Magdeburg, Magdeburg, Germany*
[b]*German Center for Neurodegenerative Diseases (DZNE), Magdeburg, Magdeburg, Germany*
[c]*Institute of Cognitive Neuroscience, University College London, London, UK*
[d]*Center for Behavioral Brain Science, Magdeburg, Germany*
[e]*Wellcome Centre for Human Neuroimaging, UCL Queen Square Institute of Neurology, University College London, London, UK*
[f]*7Lund University BioImaging Center, Lund University, Lund, Sweden*
[g]*Department of Neurology, UMC Utrecht, Utrecht University, Utrecht, The Netherlands*
[h]*Departement of Radiology, Sahlgrenska Akademy, University of Gothenburg, Gothenburg, Sweden*
[i]*NeuroSpin, CEA & Université Paris-Saclay, Gif-Sur-Yvette, France*
[j]*Sir Peter Mansfield Imaging Centre, School of Physics and Astronomy, University of Nottingham, Nottingham, UK*
[k]*Department of Radiology, University Medical Center Leiden, Leiden, The Netherlands*
[l]*Department of Clinical Neurosciences, University of Cambridge, Cambridge, UK*
[m]*Wellcome Centre for Integrative Neuroimaging, University of Oxford, Oxford, UK*
[n]*Imago 7 Research Foundation, Pisa, Italy*
[o]*Laboratory of Medical Physics and Magnetic Resonance, IRCCS Stella Maris, Pisa, Italy*
[p]*Center for Magnetic Resonance in Biology and Medicine (UMR 7339), CRMBM, CNRS - Aix Marseille Université, Marseille, France*
[q]*Physikalisch-Technische Bundesanstalt (PTB), Berlin, Germany*
[r]*Memory Clinic, Skåne University Hospital, Malmö, Sweden*
[s]*Erwin L. Hahn Institute for Magnetic Resonance Imaging, University of Duisburg-Essen, Essen, Germany*
[t]*Medical Physics in Radiology, German Cancer Research Center (DKFZ), Heidelberg, Germany*
[u]*Faculty of Physics and Astronomy and Faculty of Medicine, University of Heidelberg, Heidelberg, Germany*
[v]*Danish Center for Magnetic Resonance, Copenhagen University Hospital Hvidovre, Hvidovre, Denmark*
[w]*Department of Neurology, Copenhagen University Hospital Bispebjerg, Copenhagen, Denmark*
[x]*German Center for Neurodegenerative Diseases (DZNE), Bonn, Germany*
[y]*Center for Neuroscience Imaging Research, Institute for Basic Science and Department of Biomedical Engineering, Sungkyunkwan University, Suwon, Republic of Korea*
[z]*Techna Institute & Koerner Scientist in MR Imaging, University Health Network, Toronto, Ontario, Canada*
[aa]*Biomedical Magnetic Resonance, Otto-von-Guericke University, Magdeburg, Germany*
[bb]*Leibniz-Institute for Neurobiology (LIN), Magdeburg, Germany*

Conflicts of interest: None related to this study.

*Corresponding author. Tel.: +49 391 67 250 51; Fax: +49 391 67 250 60.
E-mail address: emrah.duezel@dzne.de

https://doi.org/10.1016/j.dadm.2019.04.010

Abstract

Introduction: The goal of European Ultrahigh-Field Imaging Network in Neurodegenerative Diseases (EUFIND) is to identify opportunities and challenges of 7 Tesla (7T) MRI for clinical and research applications in neurodegeneration. EUFIND comprises 22 European and one US site, including over 50 MRI and dementia experts as well as neuroscientists.

Methods: EUFIND combined consensus workshops and data sharing for multisite analysis, focusing on 7 core topics: clinical applications/clinical research, highest resolution anatomy, functional imaging, vascular systems/vascular pathology, iron mapping and neuropathology detection, spectroscopy, and quality assurance. Across these topics, EUFIND considered standard operating procedures, safety, and multivendor harmonization.

Results: The clinical and research opportunities and challenges of 7T MRI in each subtopic are set out as a roadmap. Specific MRI sequences for each subtopic were implemented in a pilot study presented in this report. Results show that a large multisite 7T imaging network with highly advanced and harmonized imaging sequences is feasible and may enable future multicentre ultrahigh-field MRI studies and clinical trials.

Discussion: The EUFIND network can be a major driver for advancing clinical neuroimaging research using 7T and for identifying use-cases for clinical applications in neurodegeneration.

Keywords: Magnetic resonance imaging (MRI); Ultrahigh-field MRI; Alzheimer's disease (AD); Subjective cognitive decline (SCD); Mild cognitive impairment (MCI); Parkinson's disease (PD); Vascular dementia

1. Background

Magnetic resonance imaging (MRI) measures of brain structure and function are important pillars in the assessment of dementias, both in clinical practice and for research. There is a pressing need for more sensitive and specific biomarkers of neurodegeneration, and for new approaches to study pathology and its functional consequences. MRI at ultrahigh-field strengths (at 7 Tesla, 7T) is potentially ideal in this context—it is safe, quick, and can improve sensitivity and specificity (compared with 3T MRI). With a view to realize the full potential of ultrahigh-field MRI at 7T for neurodegenerative disease research, a new working group was established in 2016: the European Ultrahigh-Field Imaging Network in Neurodegenerative Diseases (EUFIND) (Fig. 1A). It comprises imaging and dementia experts representing 22 sites across Europe, including all scanner vendors, to work together to identify opportunities and challenges of 7T MRI and draw a roadmap for implementing and harmonizing ultrahigh-field MRI methods for the in vivo assessment of neurodegenerative diseases.

The initial focus of EUFIND was Alzheimer's disease (AD), but with the inclusion of several Parkinson's disease (PD) specialists, EUFIND has extended the scope of this initiative to optimizing and harmonizing protocols with a focus on these two most common neurodegenerative disorders. EUFIND also interacts with the JPND (EU Joint Programme—Neurodegenerative Disease Research) working group for harmonizing MRI in vascular dementia (HARNESS) through members participating in both initiatives.

EUFIND's scope includes clinical applications and research using 7T MRI to (1) help disseminate knowledge across centers, (2) enable large ultrahigh-field, multisite, and multivendor studies in a harmonized network, (3) facilitate identification of clinical use-cases for 7T, and (4) calibrate methods for mapping tissue structure, function, vascularization, molecular, and metabolic status.

2. Methods

The EUFIND working group has conducted two international meetings, several telephone conferences and continued its efforts beyond the JPND funding with a third meeting in early 2018 (Fig. 1B).

During the first EUFIND meeting in Magdeburg, the working group identified 7 core subtopics and elected subtopic coordinators. A steering committee (see Appendix) was appointed comprising EUFIND coordinators, subgroup coordinators, and country representatives. Subgroup coordinators (see Appendix), together with EUFIND members interested in that subgroup (see Appendix), defined topics of interest, drafted a roadmap for addressing these topics, and optimized a scanning protocol.

During the second meeting in Leiden, subgroup coordinators presented their progress, and on the basis of each subgroup's recommendations, the first EUFIND scanning protocol was agreed. Subsequently, all site representatives expressed their interest to participate in a multicentre pilot study to test the proposed protocol, hence exceeding the original JPND project plan.

3. Results

3.1. The EUFIND network

EUFIND includes 14 sites operating Siemens 7T MRI systems, whereas 6 sites operate Philips scanners and 2 General Electric (GE). All sites, except one, are equipped with

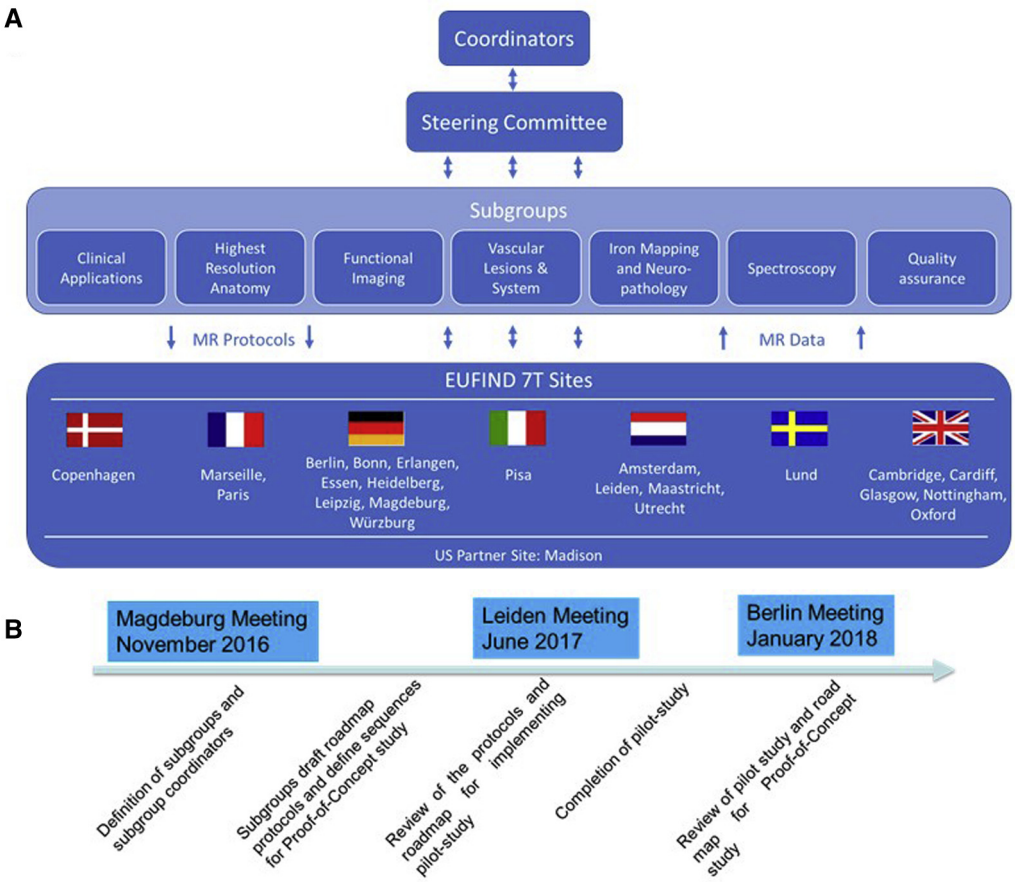

Fig. 1. (A) Structure of EUFIND. (B) Timeline of EUFIND working group meetings and milestones. Abbreviations: EUFIND, European Ultrahigh-Field Imaging Network in Neurodegenerative Diseases.

the same RF head-coil with 32 receiver channels (1 site uses a 24-channel version, Nova Medical coil). We identified several differences on the transmit side between Siemens and Philips/GE systems. Our survey also revealed gradient strengths ranging from 38 to 80 mT/m. Such hardware differences were considered when harmonizing the imaging protocols.

3.2. Subtopic results and recommendations

3.2.1. Clinical application/clinical research

The utilization of 7T in clinical practice is in its infancy. This may soon change, however, in light of the approval of the first 7T systems for clinical use (in the US and in the EU) (https://www.fda.gov/NewsEvents/Newsroom/PressAnnouncements/ucm580154.htm).

Ultra-fast acquisition: The increased signal-to-noise ratio provided by 7T MRI can be exploited for speeding-up acquisitions with image resolutions commonly used at clinical field strength (3T), thereby improving motion robustness and/or shortening the time required for imaging patients.

Clinical research: High-resolution structural imaging with 7T MRI is ideally placed to complement molecular measures of tau and amyloid pathology by providing unique information on disease staging, as suggested by the research framework for AD [1]. We have specifically identified the following topics for future clinical research:

- Disease modeling: Taking advantage of the superior spatial resolution of 7T MRI, longitudinal multiparametric high-resolution imaging could better inform mathematical models of disease progression and offer a safe and quick tool for repeat use in treatment trials.
- Functional assessment: Functional 7T MRI can reach submillimeter resolution [2,3], thereby allowing to functionally probe and assess the integrity of small anatomical structures, such as entorhinal cortex subregions, hippocampus subfields, locus coeruleus, and basal ganglia circuits. Such information would facilitate understanding of disease effect on brain functions from the earliest stages of AD and PD and to probe target engagement in drug trials.
- Nonamyloid/non–tau-pathology: High-resolution angiography at 7T can aid the detection of disease comorbidities such as vascular pathology.
- Differential diagnosis: Iron mapping with 7T MRI could help improve the differential diagnosis of neurodegenerative diseases, for example, across parkinsonian disorders.

Table 1
Sequence parameters of the high-resolution anatomical imaging protocol

	3D-MPRAGE			2D-TSE		
	Siemens	GE	Philips	Siemens	GE	Philips
Spatial resolution mm	0.65 iso	0.7 iso	0.65 iso	0.4 × 0.4 × 1.0	0.4 × 0.4 × 1.1	0.44 × 0.45 × 1.0
Nr. of slices	256	240	256	55	28 × 2	55
Repetition time ms	2500	2500	2500	8020	15,000	8000
Echo time ms	2.92	3	3.1	76	75	121
Magn. preparation	Non-sel IR	Non-sel IR	Non-sel IR	No	No	No
TI	1100 ms	600 ms	1100 ms	N.A.	N.A.	N.A.
Flip angle	7 deg	7 deg	8 deg	n/a	n/a	n/a
Acceleration factor	GRAPPA 2	ASSEST 2	SENSE 1.6 (AP)	None	2	None
Acquisition time min	8:14	6:29	8:12	7:13	6:30 × 2	8:48

Abbreviations: GE, General Electric; GRAPPA, generalized autocalibrated partially parallel acquisition; 3D-MPRAGE, 3-dimensional magnetization prepared rapid acquisition with gradient echo; 2D-TSE, 2-dimensional turbo spin echo.

- End-point markers for clinical trials: Increased sensitivity to quantify neurodegeneration could offer a validated readout for use in controlled designs.

Diagnostic imaging: EUFIND is the ideal framework to identify the most promising applications of 7T MRI in clinical neurology; with most participating sites embedded in a clinical setting, direct comparisons with routine 3T assessments are feasible. We do not expect 7T MRI to replace established molecular imaging, that is, positron emission tomography, or cerebrospinal fluid biomarkers, of neurodegenerative diseases. However, existing evidence suggests that 7T MRI could (1) be more sensitive to early neurodegeneration in prodromal/preclinical states of neurodegenerative diseases, (2) offer a highly sensitive tool for the detection of vascular pathology, and (3) improve target placement for noninvasive brain stimulation techniques. EUFIND could also help identify in epilepsy more subtle lesions than 3T MR even though this latter topic is not in the immediate scope of EUFIND.

3.2.2. *Highest resolution anatomy*

7T MRI offers superior anatomical resolution over lower field strengths. To illustrate this, we imaged and segmented medial temporal lobe regions. As illustrated in recently developed 7T segmentations protocols for the medial temporal lobe [4], certain key landmarks that are difficult to identify at 3T, such as the endfolial pathway distinguishing dentate gyrus from hippocampal subfield CA3, can be reliably identified in 7T scans. Two high-resolution anatomical sequences were successfully implemented and analyzed at 13 EUFIND sites: a T1-weighted sequence for whole-brain anatomy (3-dimensional magnetization prepared rapid acquisition with gradient echo, 0.65-mm isotropic resolution), and a T2-weighted acquisition centered on the medial temporal lobe (2D Turbo-Spin Echo, 0.4 × 0.4 × 1.0 mm resolution, orthogonal to the hippocampus' longest axis). Table 1 summarizes the acquisition details for each of the sequences. Protocols for different vendors were largely analogous—but minor differences existed. We have not used dielectric pads to improve signal from the medial temporal lobes because these were not available at all sites, are not approved for clinical use and raise safety concerns because of their considerable effects on the local specific adsorption rate. Data were acquired from 22 healthy volunteers, scanned across all 13 sites.

Whole-brain T1 scans were bias-corrected [5] before segmentation using Freesurfer's "recon-all" pipeline [6]. Hippocampal subfield segmentation was undertaken using the automated segmentation of hippocampal subfields protocol package (https://sites.google.com/site/hipposubfields/) in combination with the Magdeburg 7T atlas, which was created using a recently published subfield segmentation protocol [4]. Fig. 2A highlights the importance of bias-field correction to provide spatially homogenous images for whole-brain segmentation (Fig. 2B). Fig. 3 illustrates the interscanner consistency of hippocampal segmentation from T2-weighted images.

In conclusion, whole-brain T1-weighted and high-resolution T2-weighted sequences were successfully implemented and analyzed across sites and vendors. These initial efforts revealed two acquisition problems, namely excessive head motion and signal loss in the inferior temporal lobe on T2-weighted scans. Future solutions could include prospective motion correction [7] and utilization of parallel transmission to homogenize the transmit field [8].

3.2.3. *Functional imaging*

The main advantages of higher field strength for fMRI are the increased nuclear magnetization and susceptibility effects, leading to increased blood oxygenation level-dependent contrast [9,10]. However, acquisition of fMRI data suffers from physiology- and hardware-related challenges that may impair the generalization of fMRI studies across imaging platforms [11]. We thus evaluated the feasibility of a standardized protocol across several 7T sites for resting-state fMRI in neurodegenerative diseases. In the preclinical course of AD, tau-pathology spreads from perirhinal and entorhinal cortex to hippocampal subfields and amygdala and later to other cortical temporal regions, to frontal and midline parietal

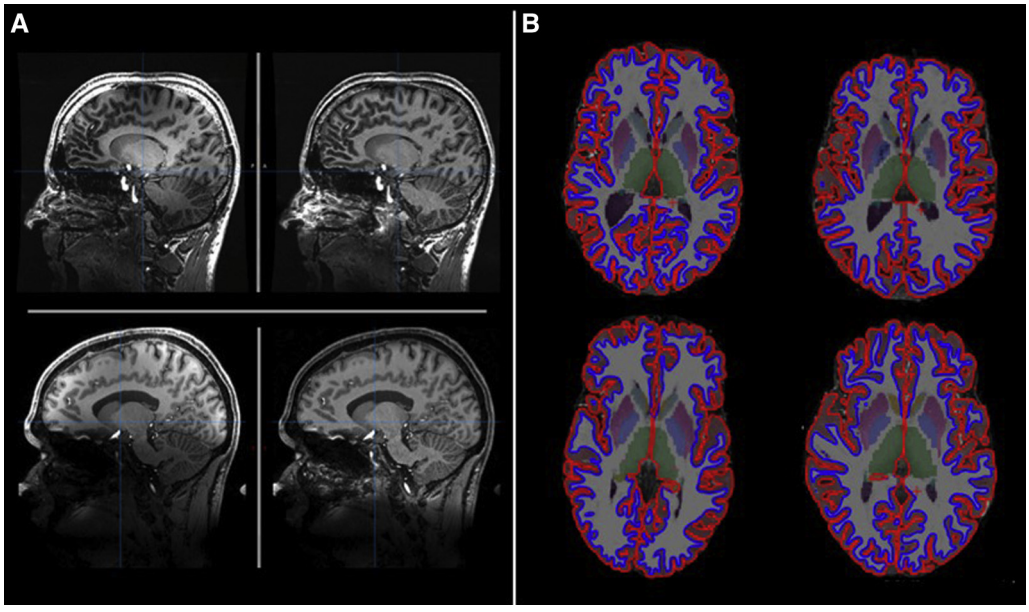

Fig. 2. Sample T1-weighted scans and Freesurfer segmentation across sites. (A) Sample T1-weighted scans from two different sites (top: Pisa [GE], bottom: Bonn [Siemens]). Left: original data; right: after bias-field correction. (B) Sample Freesurfer segmentation results from four sites (top left: Bonn, top right: Essen, bottom left: Magdeburg, bottom right: Paris).

regions [12–14]. Therefore, tools to assess the detailed functional connectivity profile of the perirhinal cortex (PRC) in preclinical AD would be valuable. We assessed whether PRC functional connectivity with the entorhinal cortex, hippocampal subfields, and cortical regions could be reliably delineated in multisite resting-state data and could be distinguished from connectivity patterns of the parahippocampal cortex. This comparison is relevant because the parahippocampal cortex (PHC) is affected in later stages of tau-progression than the PRC [15]. PHC and PRC seed regions were selected to analyze resting-state data as used to investigate the integrity of entorhinal and hippocampal subregional connectivity [16]. fMRI data were acquired at five different imaging sites for a total of eight subjects (see sequence parameters in Table 2 and Figs. 4 and 5). Seed-to-voxel correlational analyses using PRC or PHC seeds were performed on the distortion and motion corrected fMRI data using the CONN toolbox [17]. As covariates, white matter and cerebrospinal fluid time series and subjects' realignment parameters were included to account for physiological noise and motion, respectively. For group analysis, correlation maps were registered to the MNI atlas and averaged across subjects.

For all subjects, the seed ROI's could be reliably obtained and analyzed. Although both seed-regions are located in close proximity, the observed correlation maps exhibited clearly distinct patterns in agreement with earlier studies [16], with no large differences across sites and subjects, demonstrating the feasibility of functional connectivity multicentre studies using 7T fMRI.

Because this proof-of-concept study focused on feasibility, we used an anatomically narrow acquisition protocol limited to the medial temporal lobe. It would be meaningful to include cortical regions such as parietal and midline regions in future protocols.

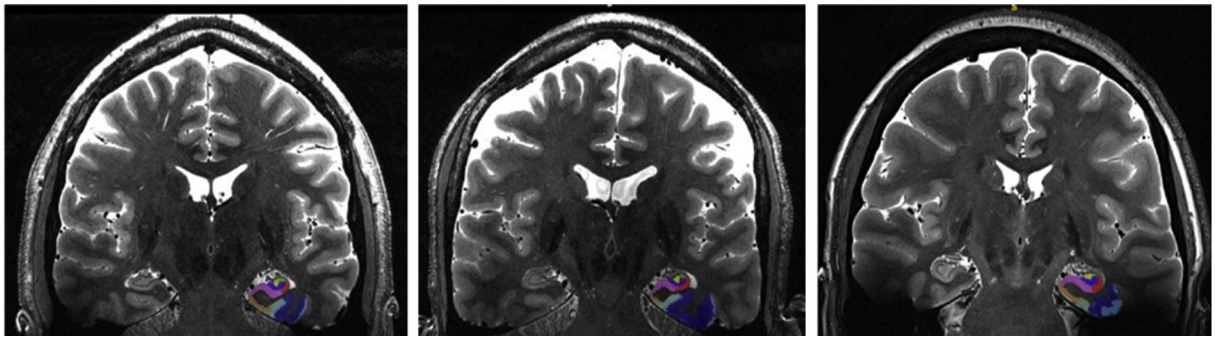

Fig. 3. Sample T2-weighted coronal MRI scans through the body of the hippocampus and adjacent medial temporal lobe structures, immediately posterior to the hippocampal head (uncal apex). Scans acquired from Leipzig (left), Magdeburg (center), and Paris (right). Color legend of segmented regions: Brodmann area 36—dark blue, area 35—turquoise, entorhinal cortex—brown, subiculum—mauve, CA1—red, CA2—green, CA3—yellow, dentate gyrus—blue. The segmentation is based on a new protocol by Berron et al. [4].

Table 2
Sequence parameters of the resting-state fMRI protocol

	Resting-state fMRI		
	Siemens	GE	Philips
Spatial resolution mm	1.1 iso	1.1 iso	1.1 iso
Nr. of slices	40	40	40
Nr. of volumes	250	240	200 + 4 dummies
Repetition time ms	2400	3000	3000
Echo time ms	22	22.5	22
Partial Fourier	6/8	Off	Off
Acceleration factor	GRAPPA 4	ASSET 3	GRAPPA 4
References lines	64	64	64
Acquisition time min	10:27	12:12	10:12

Abbreviations: GE, General Electric; GRAPPA, generalized autocalibrated partially parallel acquisition.

3.2.4. *Vascular system/vascular pathology*

7T MRI offers several unique opportunities to further our understanding of vascular contributions to neurodegenerative diseases. This includes both functional and structural assessment of the brain vasculature and parenchyma, as well as perfusion [18,19].

7T MRI allows for high-resolution imaging of both the arteries [18,20] (time of flight) and the veins [19,21] (T2* weighted imaging/susceptibility weighted imaging). Postprocessing techniques are being developed for quantitative measures of vessel density, length, tortuosity, and branching patterns. In addition, structural features of the wall of intracranial vessels can be assessed (reviews: [18,22]), although this is currently still limited to larger vessels (circle of Willis and a few major branches) [e.g., [23]]. Apart from measures of vessel structure, different aspects of vascular function, including blood flow, pulsatility of flow in small penetrating arteries—a possible indicator of vascular stiffness—[24,25], vascular reactivity to vasoactive agents (e.g., carbon dioxide) or neuronal stimulation (i.e., fMRI), can be assessed with 7T MRI at a level of spatial and temporal resolution that markedly exceeds lower field strength MRI [18,26]. Finally, 7T also offers new perspectives on the consequences of vascular disease in the parenchyma. Methods have been developed to detect cortical microinfarcts [27,28], and to improve detection of microbleeds [29,30] and secondary neurodegeneration [31].

We attempted to harmonize a recently published 2D phase-contrast sequence to measure pulsatility in perforating arteries of the white matter in the semioval center [25]. We found, however, large sensitivity differences across scanner platforms in detecting perforating arteries. Such performance inconsistencies warrant future study, and illustrate in exemplary fashion the challenges of harmonization. The method was thus applied to the larger perforating arteries in the basal ganglia. Eleven 2D phase-contrast scans were available from 7 sites (all three scanner vendors included) and were successfully analyzed. The results (data not shown) confirmed the values from the first publication [25].

3.2.5. *Iron mapping and neuropathology detection*

Iron dysregulation is thought to play a significant role in the pathogenesis of neurodegenerative diseases such as AD [32], PD [33], and amyotrophic lateral sclerosis [34]. Large numbers of iron-laden glial cells are commonly found in the vicinity of pathological aggregates in these disorders

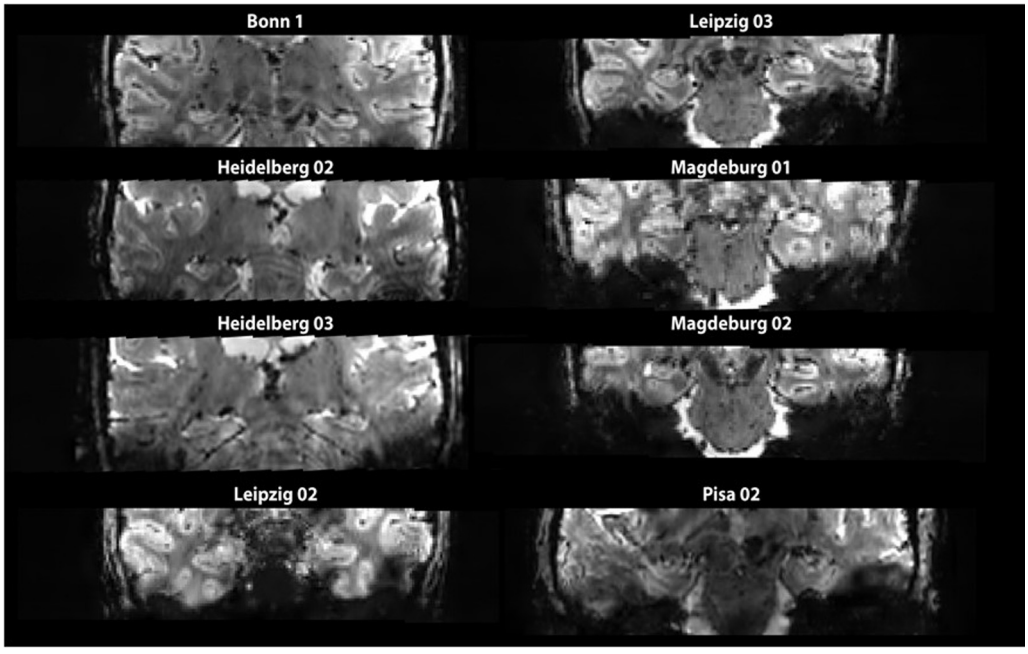

Fig. 4. Overview of subjects' mean EPI from different sites.

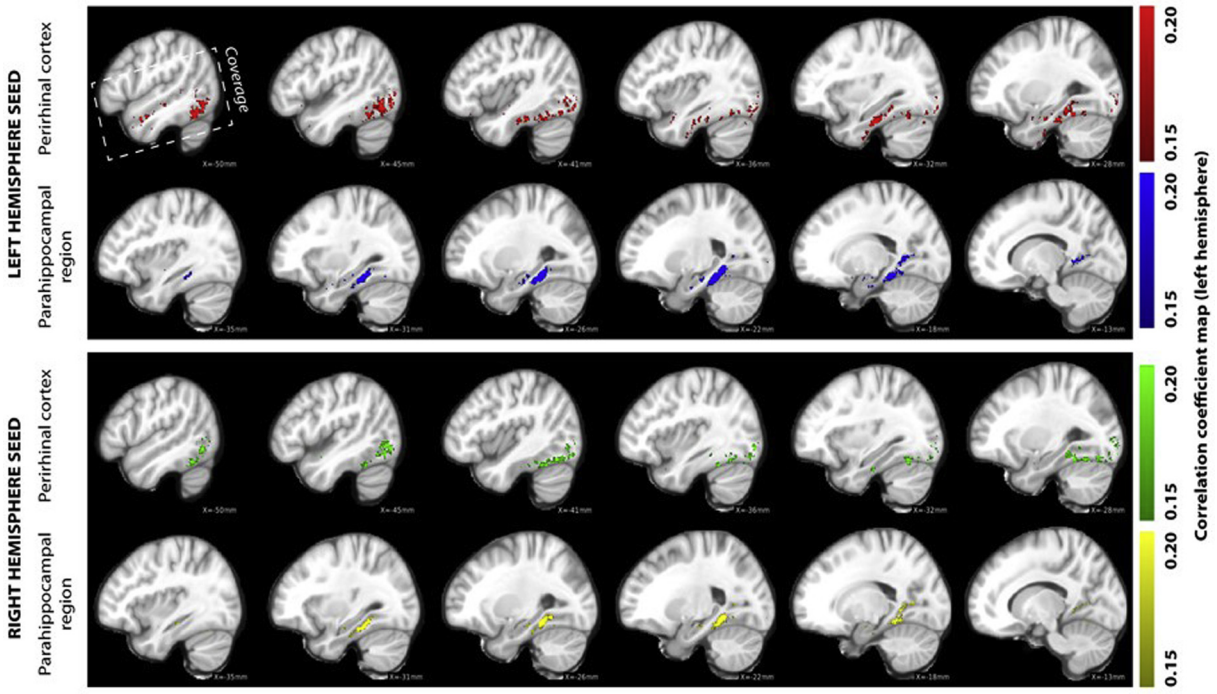

Fig. 5. Average functional correlation coefficient maps. Each seed region is color-coded (left hemisphere perirhinal cortex and parahippocampal region: red and blue, respectively, and green and yellow for the right hemisphere, respectively).

[35–40]. Quantitative susceptibility mapping (QSM) [41] and apparent transverse relaxation rate (R2*)—both related to brain iron levels in vivo—revealed differential patterns of involvement in aging [42–46] and AD [47–49], PD [50–52], and amyotrophic lateral sclerosis [53–55]. In light of this, EUFIND has carried out a systematic calibration study of QSM and R2* measurements from multiple sites using scanners from all three vendors (see Table 3 for Siemens scanners).

Single- and multi-echo data sets, scanned at six different sites, were preliminarily investigated [54]. QSM and R2* reconstructions were performed successfully from all data sets. Moderate subject motion was observed in one-third of scans. However, a subsequent experiment focusing on the striatum, with the prediction that magnetic susceptibility must increase as a function of age, returned a qualitatively positive result (Fig. 6).

In conclusion, multisite and multi-vendor QSM and R2* were reliably reconstructed at 7T. Despite the presence of motion artifacts in some data sets [56], aging effects were detectable visually.

Table 3
Sequence parameters for QSM

	QSM		
	Siemens	GE	Philips
Spatial resolution mm	0.3 × 0.3 × 1.25	0.4 × 0.4 × 1.2	0.35 × .035 × 1.25
Nr. of slices	120	136	120
Repetition time ms	18	18.5	18
Echo time ms	10	10	10
Phase—Partial Fourier	7/8	OFF	OFF
Slice—Partial Fourier	7/8	OFF	OFF
Acceleration factor	GRAPPA 2	ASSET 2	SENSE 2.1
Acquisition time min	8:46	9:08	7:50

Abbreviations: GE, General Electric; GRAPPA, generalized autocalibrated partially parallel acquisition; QSM, quantitative susceptibility mapping.

3.2.6. *Spectroscopy*

In vivo MR spectroscopy (MRS) [57] and CEST spectroscopy [58] can noninvasively quantify a portion of the biochemical composition of living tissue. Preclinical MRS markers for neurodegenerative disease may complement structural and functional imaging readouts [59]. Proton (1H) MRS has reached the arena of clinical research both because of its ability to detect and quantify several human metabolites in vivo, with sequences in principle available on all clinical MRI systems. A recent multicentre proton MRS reproducibility study using four 7T systems has reported an acceptable reproducibility level for MRS data across centers and vendors [60]. We hereby present additional normative MRS data across three of the participating sites (single vendor). Data were acquired from a 2 × 2 × 2 cm^3 volume centered on the posterior cingulate cortex using the same MRS pulse sequence across all three sites. The data returned a high level of reproducibility for a broad range of metabolites (Fig. 7).

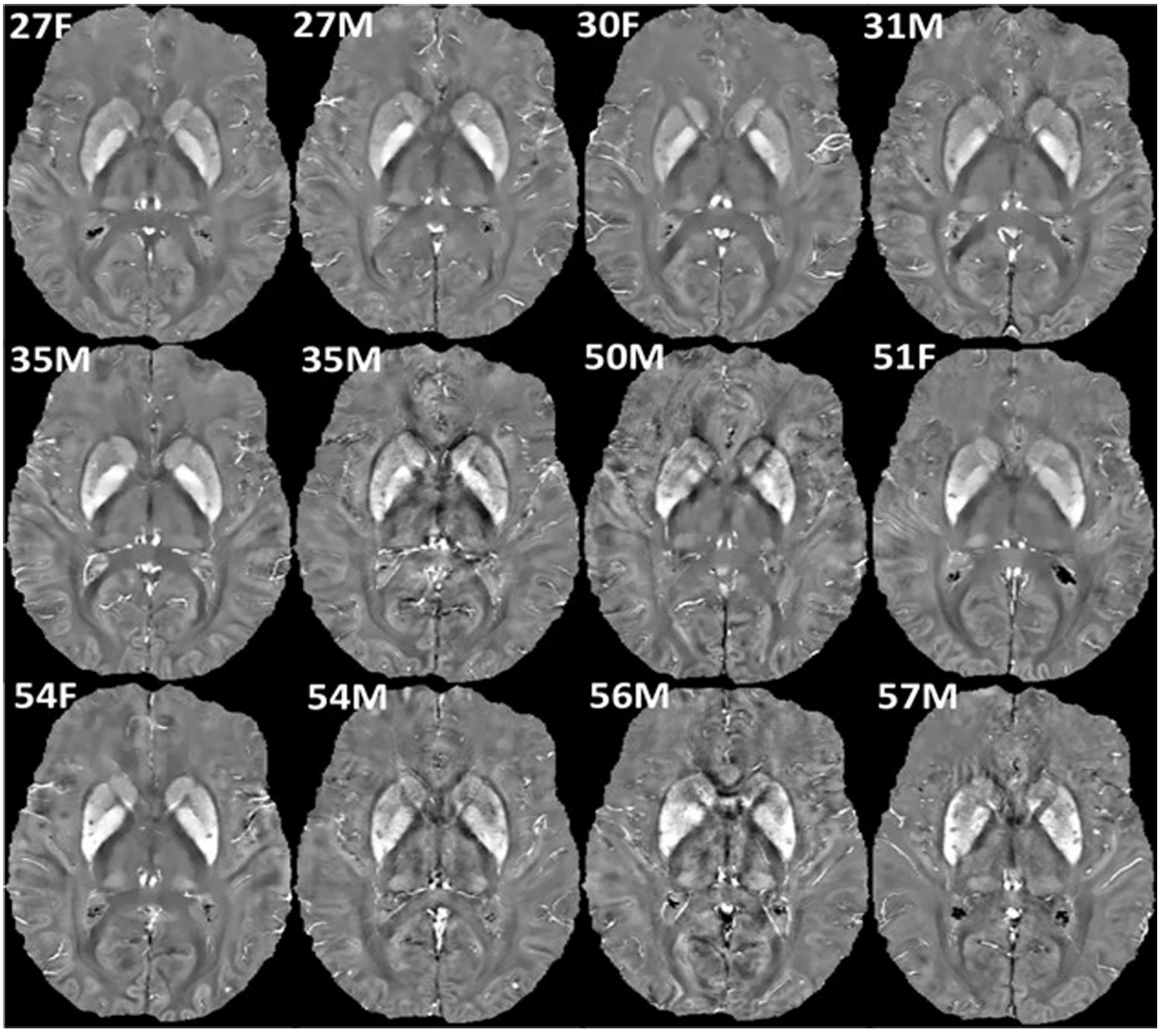

Fig. 6. Axial cuts through the corpus striatum illustrating visually tractable QSM-age dependencies. QSM from all scanner vendors were included. The QSM windowing range was (−0.1, 0.1) in parts per million [M: Male, F: Female]. Abbreviation: QSM, quantitative susceptibility mapping.

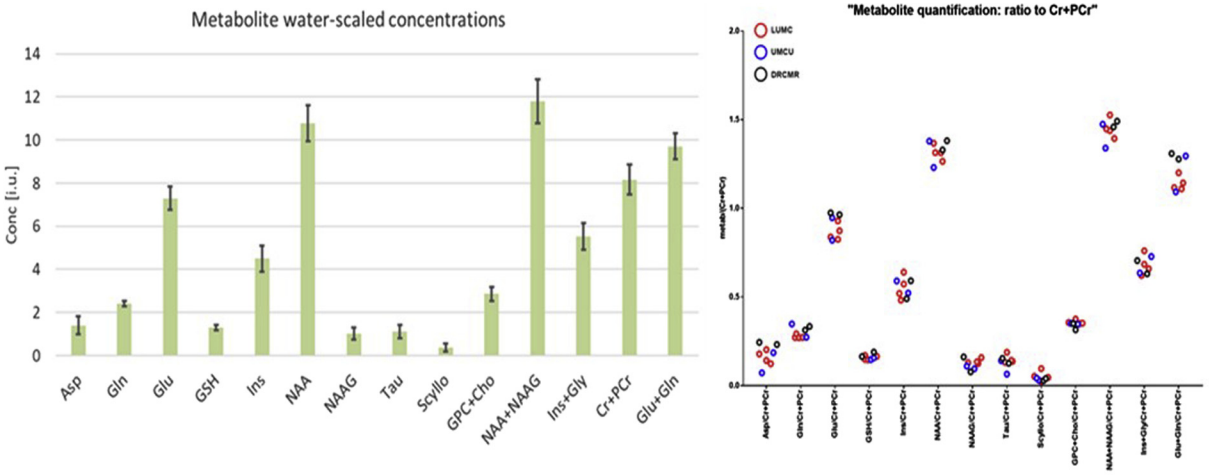

Fig. 7. Left: average and standard deviations of metabolite concentrations acquired at the three 7T MR scanners; right: scatter plot of all individual data (8 subjects) presented as ratios to total creatine.

3.2.7. Quality assurance (QA), standard operating procedures (SOPs), safety, and multivendor harmonization

Harmonization of imaging protocols, SOPs, and common quality assessment are key to enable 7T MRI for future use in multicentre trials. The main challenges working toward these goals are the following:

1. Working across institutions: The implementation of SOPs relies heavily on how these interface with the working practices of the individual institution. SOPs need to be sufficiently detailed to enable consistency, whereas sufficiently flexible to allow local working practices to be implemented without significant extra resource.
2. Working across vendors: Attempts to standardize protocols for imaging and quality assurance need to consider the limitations of each vendor's image acquisition and reconstruction frameworks, without necessarily accepting a "lowest common denominator" solution.
3. Working across regulatory bodies: Scanning at 7T poses some safety concerns where the potential risks are not always known. Because safety is overseen by different regulatory bodies in different institutions, regions, and countries, a common policy is not easy to achieve.

Work in addressing these has already begun within specific national networks, and EUFIND closely collaborates with these national networks and enhances communication between them. This is enabled by shared PIs across these networks within EUFIND.

3.2.8. German Ultrahigh-Field Imaging (GUFI) network

The GUFI network was founded at the end of 2013 supported by the German Research Foundation. System reproducibility in human subjects has been compared within the network to validate multicentre brain imaging at 7T, known as the "traveling heads" study [61]. High reproducibility was found across all sites, but differences in intersite versus intrasite reproducibility were identified and assigned to hardware differences.

GUFI has implemented a common QA protocol to assess system performance based on signal-to-noise ratio, B1+, noise, and stability measures. High agreement was found between sites, but the protocol also revealed hardware and calibration faults at some sites that were previously undetected.

GUFI partners have tried to clarify ethical, regulatory, liability, and safety issues common to all 7T MR sites. To date, very few medical implants have been certified as MR-conditional at 7T. GUFI partners defined and published a consensus recommendation for dealing with passive implants, including a standardized decision-making process regarding whether a measurement at 7T can be performed safely [62]. The network is currently establishing a database with information on implant safety to share knowledge and experience on this topic. In addition, online safety training accepted by all sites has been implemented.

3.2.9. UK7T network

Established in 2015 and funded by the UK Medical Research Council, this network aims to develop a platform for multicentre trials at 7T, enable multivendor studies and produce "work-horse" protocols. In a similar way to GUFI, the UK7T network has carried out a "traveling head" study with 10 participants across 5 sites, using a range of harmonized protocols including structural and functional measures. Initial data show that, as well as matching protocol parameters as much as possible, it is essential to standardize the various calibration steps (transmit power, B0 shim), to improve uniformity [63]. At present, QA procedures and a common phantom are also being disseminated among the UK7T partners.

3.2.10. Future directions: the EUFIND protocol

On the basis of the available hardware and the recommendations from each subtopic, we developed a EUFIND 7T high-resolution imaging protocol. This protocol combines structural imaging sequences for morphometric information (structural T1 and T2 sequences), a sequence to image vascular pulsatility (2D phase), a resting-state fMRI sequence, and an iron-sensitive 3D gradient echo sequence for QSM. The details of the protocol are given in Table 4.

The results from the pilot study showed overall good image quality across sites and vendors but also revealed that protocol harmonization needs further improvements, especially regarding transmitter calibration.

4. Discussion

The EUFIND subgroups were ambitious in exploring the capabilities of 7T MRI technology. Indeed, the protocol resulting from subgroup recommendations goes beyond what can be achieved by 3T MRI. The group identified and focused on methods with the highest potential for use in neurodegenerative diseases and agreed not to focus on areas where the benefit of high field strength is currently less certain, for example, diffusion MRI.

From the subgroup reports, it became apparent that each MRI modality posed a different set of challenges in multivendor harmonization. Whereas high-resolution anatomical

Table 4
The EUFIND multisite protocol

	Resolution (mm^3)	Acquisition time (min:sec)
T1 MPRAGE	0.65 isotropic	8:14
2D phase-contrast	.3 × .3 × 2	~5:00
Resting-state fMRI - inverted phase encoding	1.1 isotropic	0:24
Resting-state fMRI	1.1 isotropic	10:27
Quantitative susceptibility mapping	.35 × .35 × 1.25	8:46
T2 TSE hippocampal angulated	.4 × .4 × 1	7:47

Abbreviation: MPRAGE, magnetization prepared rapid acquisition with gradient echo.

imaging and QSM sequences were relatively straightforward to translate across vendors, unforeseen limitations precluded full harmonization of vessel pulsatility measurements and spectroscopy. Solutions may require additional contributions and developments by scanner vendors.

Thirteen 7T sites implemented the recommended protocol (Table 4 for acquisition details) and provided healthy volunteer data within the very short time frame of the JPND project. For the first time, 7T MRI data acquired on scanners from all vendors across multiple countries were assessed in a single study. We consider this alone to be a success given that conducting such a study went far beyond the original scope of the working group, and several sites had only recently received their scanner hardware or had a major focus on other organ systems. These sites have nonetheless made substantial progress in adopting the joint protocol, and expect that the full network will soon be able to join the EUFIND roadmap implementation.

The pilot study demonstrated that harmonizing 7T MRI data acquisition protocols across institutions, system vendors, and regulatory bodies is viable. It was also successful in revealing specific problems and challenges of multisite 7T imaging, which can now be effectively addressed. To that end, it also helped to establish data exchange and communication channels across sites, and identified subgroup-specific expertise in sequence implementation and data analysis. We believe that this will enable EUFIND to advance the implementation of technology for addressing challenges of 7T imaging such as reducing movement-related artifacts at high resolution.

EUFIND has thus laid the foundation to apply 7T in multisite research studies in Europe. One of the obvious questions to address in the near term is how much added benefit 7T technology provides in a head-to-head comparison with 3T technology for improving research and clinically relevant personalized medicine approaches. For AD, one hypotheses would be that ultrahigh resolution imaging at 7T improves on current 3T imaging of brain structure, function, and vasculature for individualized precision medicine for early assessment and prevention of AD. Addressing this hypothesis will require (1) to identify the added sensitivity of ultrahigh resolution structural imaging at 7T for detecting and quantifying progressive neurodegeneration in aging and preclinical/prodromal AD as compared with currently available protocols at 3T, (2) to determine whether the trajectory of cognitive change is explained better by ultrahigh resolution measures of atrophy than the current 3T standard, (3) to identify neural dysfunction in small brain networks that are affected early in disease (i.e., subregions of the entorhinal cortex, the locus coeruleus), (4) to determine to what extent brain dysfunction is related to neurodegeneration, (5) to identify the contribution of small-vessel related vascular risk factors to neurodegeneration and brain dysfunction.

With EUFIND, we have established a network that enables addressing these topics in the near future. We emphasize that the increased signal-to-noise ratio provided by 7T MRI can also be exploited for speeding-up acquisitions with image resolutions commonly used at clinical field strength (3T), thereby improving motion robustness and/or shortening the time required for imaging patients, as opposed to improving resolution.

Acknowledgments

This publication is an outcome of an EU Joint Programme—Neurodegenerative Disease Research (JPND) working group (see www.jpnd.eu). The working group was supported through the German Federal Ministry of Education and Research (BMBF, funding code 01ED1620) under the aegis of JPND. E Düzel receives funding from the Human Brain Project (European Union's Horizon 2020 research and Innovation Program under specific grant agreement No. 720270, SGA1/2, SP3, WP 3.3.1), DFG (SFB 779, A07), DFG (SFB 1315, B06) and the MRC (Project 538374 F69 to E Düzel). The Wellcome Centre for Human Neuroimaging is supported by core funding from the Wellcome (203147/Z/16/Z). JBR is supported by the Wellcome Trust (103838) and Medical Research Council (SUAG/004/91365). The research of Jeroen Hendrikse has received funding from the European Research Council under the European Union's Horizon 2020 Program (H2020)/ERC grant agreement n°637024 (HEARTOFSTROKE) and H2020 grant agreement No 666881, SVDs@target. Jeroen Hendrikse is supported by the Netherlands Organization for Scientific Research (NWO) under grant n°91712322. The research of Jaco Zwanenburg has received funding from the European Research Council under the European Union's Seventh Framework Program (FP7/2007-2013)/ERC grant agreement n°337333 (SmallVesselMRI).The UK7T Network is funded by MRC Partnership Grant MR/N008537/1.
The Wellcome Centre for Integrative Neuroimaging is supported by core funding from the Wellcome Trust (203139/Z/16/Z). CRMBM 7T program received funding from France Life Imaging (ANR-11-INBS-0006), Investissements d'Avenir (ANR-11-EQPX-0001), Aix-Marseille University Excellence Initiative A*MIDEX (grant ANR-11-IDEX-0001-02).
Mark E. Ladd and Oliver Speck acknowledge support from the German Research Foundation (DFG) for funding of the German Ultrahigh Field Imaging (GUFI) network, grant no. LA 1325/7-1 and SP 632/9-1.
Authors' contributions: The authors contributed according to their role in the EUFIND consortium as outlined in the Appendix.

Supplementary Data

Supplementary data related to this article can be found at https://doi.org/10.1016/j.dadm.2019.04.010.

RESEARCH IN CONTEXT

1. Systematic review: The authors reviewed the literature using traditional (e.g., PubMed) sources and meeting abstracts and presentations. Ultrahigh-field imaging at 7 Tesla in neurodegenerative diseases is an emerging field and considerable advances have recently been made concerning various 7T imaging modalities and in multisite harmonization, quality control, and safety recommendations. These relevant studies are appropriately cited.
2. Interpretation: Our work indicates that a large consortium of 7T sites to address clinically and scientifically relevant questions in neurovegetative diseases with advanced and harmonized imaging sequences is feasible.
3. Future directions: We propose a roadmap for the future of 7T imaging in neurodegenerative disease covering clinical and research topics. The increasing number of 7T sites with access to clinical populations also makes it feasible that 7T imaging can be used in multicenter clinical trials.

References

[1] Jack CR Jr, Bennett DA, Blennow K, Carrillo MC, Dunn B, Haeberlein SB, et al. NIA-AA Research Framework: Toward a biological definition of Alzheimer's disease. Alzheimers Dement 2018;14:535–62.

[2] Koster R, Chadwick MJ, Yi C, Berron D, Banino A, Düzel E, et al. Big-Loop Recurrence within the Hippocampal System supports Integration of Information across Episodes. Neuron 2018;99:1342–1354.e6.

[3] Maass A, Schutze H, Speck O, Yonelinas A, Tempelmann C, Heinze HJ, et al. Laminar activity in the hippocampus and entorhinal cortex related to novelty and episodic encoding. Nat Commun 2014;5:5547.

[4] Berron D, Vieweg P, Hochkeppler A, Pluta JB, Ding SL, Maass A, et al. A protocol for manual segmentation of medial temporal lobe subregions in 7 Tesla MRI. Neuroimage Clin 2017;15:466–82.

[5] Vovk U, Pernus F, Likar B. A review of methods for correction of intensity inhomogeneity in MRI. IEEE Trans Med Imaging 2007;26:405–21.

[6] Reuter M, Schmansky NJ, Rosas HD, Fischl B. Within-subject template estimation for unbiased longitudinal image analysis. Neuroimage 2012;61:1402–18.

[7] Maclaren J, Herbst M, Speck O, Zaitsev M. Prospective motion correction in brain imaging: a review. Magn Reson Med 2013;69:621–36.

[8] Gras V, Boland M, Vignaud A, Ferrand G, Amadon A, Mauconduit F, et al. Homogeneous non-selective and slice-selective parallel-transmit excitations at 7 Tesla with universal pulses: A validation study on two commercial RF coils. PLoS One 2017;12:e0183562.

[9] Pohmann R, Speck O, Scheffler K. Signal-to-noise ratio and MR tissue parameters in human brain imaging at 3, 7, and 9.4 tesla using current receive coil arrays. Magn Reson Med 2016;75:801–9.

[10] Uludag K, Muller-Bierl B, Ugurbil K. An integrative model for neuronal activity-induced signal changes for gradient and spin echo functional imaging. Neuroimage 2009;48:150–65.

[11] Ugurbil K. Imaging at ultrahigh magnetic fields: History, challenges, and solutions. Neuroimage 2018;168:7–32.

[12] Braak H, Del Tredici K. The preclinical phase of the pathological process underlying sporadic Alzheimer's disease. Brain 2015;138:2814–33.

[13] Erdem A, Yasargil G, Roth P. Microsurgical anatomy of the hippocampal arteries. J Neurosurg 1993;79:256–65.

[14] Maass A, Lockhart SN, Harrison TM, Bell RK, Mellinger T, Swinnerton K, et al. Entorhinal tau pathology, episodic memory decline, and neurodegeneration in aging. J Neurosci 2018;38:530–43.

[15] Maass A, Landau S, Baker SL, Horng A, Lockhart SN, La Joie R, et al. Comparison of multiple tau-PET measures as biomarkers in aging and Alzheimer's disease. Neuroimage 2017;157:448–63.

[16] Maass A, Berron D, Libby LA, Ranganath C, Duzel E. Functional subregions of the human entorhinal cortex. Elife 2015;4.

[17] Whitfield-Gabrieli S, Nieto-Castanon A. Conn: a functional connectivity toolbox for correlated and anticorrelated brain networks. Brain Connect 2012;2:125–41.

[18] Zwanenburg JJM, van Osch MJP. Targeting Cerebral Small Vessel Disease With MRI. Stroke 2017;48:3175–82.

[19] De Guio F, Vignaud A, Ropele S, Duering M, Duchesnay E, Chabriat H, et al. Loss of venous integrity in cerebral small vessel disease: a 7-T MRI study in cerebral autosomal-dominant arteriopathy with subcortical infarcts and leukoencephalopathy (CADASIL). Stroke 2014;45:2124–6.

[20] Spallazzi M, Dobisch L, Becke A, Berron D, Stucht D, Oeltze-Jafra S, et al. Hippocampal vascularization patterns: a high-resolution 7 Tesla time-of-flight magnetic resonance angiography study. Neuroimage Clin 2019;21:101609.

[21] Kuijf HJ, Bouvy WH, Zwanenburg JJ, Razoux Schultz TB, Viergever MA, Vincken KL, et al. Quantification of deep medullary veins at 7 T brain MRI. Eur Radiol 2016;26:3412–8.

[22] Dieleman N, van der Kolk AG, Zwanenburg JJ, Harteveld AA, Biessels GJ, Luijten PR, et al. Imaging intracranial vessel wall pathology with magnetic resonance imaging: current prospects and future directions. Circulation 2014;130:192–201.

[23] Lindenholz A, van der Kolk AG, Zwanenburg JJM, Hendrikse J. The Use and Pitfalls of Intracranial Vessel Wall Imaging: How We Do It. Radiology 2018;286:12–28.

[24] Geurts L, Biessels GJ, Luijten P, Zwanenburg J. Better and faster velocity pulsatility assessment in cerebral white matter perforating arteries with 7T quantitative flow MRI through improved slice profile, acquisition scheme, and postprocessing. Magn Reson Med 2018;79:1473–82.

[25] Bouvy WH, Geurts LJ, Kuijf HJ, Luijten PR, Kappelle LJ, Biessels GJ, et al. Assessment of blood flow velocity and pulsatility in cerebral perforating arteries with 7-T quantitative flow MRI. NMR Biomed 2016;29:1295–304.

[26] Geurts LJ, Bhogal AA, Siero JCW, Luijten PR, Biessels GJ, Zwanenburg JJM. Vascular reactivity in small cerebral perforating arteries with 7T phase contrast MRI - A proof of concept study. Neuroimage 2018;172:470–7.

[27] Jouvent E, Poupon C, Gray F, Paquet C, Mangin JF, Le Bihan D, et al. Intracortical infarcts in small vessel disease: a combined 7-T postmortem MRI and neuropathological case study in cerebral autosomal-dominant arteriopathy with subcortical infarcts and leukoencephalopathy. Stroke 2011;42:e27–30.

[28] van Veluw SJ, Shih AY, Smith EE, Chen C, Schneider JA, Wardlaw JM, et al. Detection, risk factors, and functional consequences of cerebral microinfarcts. Lancet Neurol 2017;16:730–40.

[29] Conijn MM, Geerlings MI, Biessels GJ, Takahara T, Witkamp TD, Zwanenburg JJ, et al. Cerebral microbleeds on MR imaging: comparison between 1.5 and 7T. AJNR Am J Neuroradiol 2011;32:1043–9.

[30] Kuijf HJ, de Bresser J, Geerlings MI, Conijn MM, Viergever MA, Biessels GJ, et al. Efficient detection of cerebral microbleeds on 7.0 T MR images using the radial symmetry transform. Neuroimage 2012;59:2266–73.
[31] De Guio F, Reyes S, Vignaud A, Duering M, Ropele S, Duchesnay E, et al. In vivo high-resolution 7 Tesla MRI shows early and diffuse cortical alterations in CADASIL. PLoS One 2014;9:e106311.
[32] Smith MA, Harris PL, Sayre LM, Perry G. Iron accumulation in Alzheimer disease is a source of redox-generated free radicals. Proc Natl Acad Sci U S A 1997;94:9866–8.
[33] Sian-Hulsmann J, Mandel S, Youdim MB, Riederer P. The relevance of iron in the pathogenesis of Parkinson's disease. J Neurochem 2011; 118:939–57.
[34] Lovejoy DB, Guillemin GJ. The potential for transition metal-mediated neurodegeneration in amyotrophic lateral sclerosis. Front Aging Neurosci 2014;6:173.
[35] Brettschneider J, Del Tredici K, Toledo JB, Robinson JL, Irwin DJ, Grossman M, et al. Stages of pTDP-43 pathology in amyotrophic lateral sclerosis. Ann Neurol 2013;74:20–38.
[36] Braak H, Braak E. Neuropathological stageing of Alzheimer-related changes. Acta Neuropathol 1991;82:239–59.
[37] Braak H, Ghebremedhin E, Rub U, Bratzke H, Del Tredici K. Stages in the development of Parkinson's disease-related pathology. Cell Tissue Res 2004;318:121–34.
[38] McGeer PL, Itagaki S, Akiyama H, McGeer EG. Rate of cell death in parkinsonism indicates active neuropathological process. Ann Neurol 1988;24:574–6.
[39] Kwan JY, Jeong SY, Van Gelderen P, Deng HX, Quezado MM, Danielian LE, et al. Iron accumulation in deep cortical layers accounts for MRI signal abnormalities in ALS: correlating 7 tesla MRI and pathology. PLoS One 2012;7:e35241.
[40] Connor JR, Snyder BS, Beard JL, Fine RE, Mufson EJ. Regional distribution of iron and iron-regulatory proteins in the brain in aging and Alzheimer's disease. J Neurosci Res 1992;31:327–35.
[41] Wang Y, Liu T. Quantitative susceptibility mapping (QSM): Decoding MRI data for a tissue magnetic biomarker. Magn Reson Med 2015; 73:82–101.
[42] Daugherty AM, Haacke EM, Raz N. Striatal iron content predicts its shrinkage and changes in verbal working memory after two years in healthy adults. J Neurosci 2015;35:6731–43.
[43] Callaghan MF, Freund P, Draganski B, Anderson E, Cappelletti M, Chowdhury R, et al. Widespread age-related differences in the human brain microstructure revealed by quantitative magnetic resonance imaging. Neurobiol Aging 2014;35:1862–72.
[44] Li W, Wu B, Batrachenko A, Bancroft-Wu V, Morey RA, Shashi V, et al. Differential developmental trajectories of magnetic susceptibility in human brain gray and white matter over the lifespan. Hum Brain Mapp 2014;35:2698–713.
[45] Betts MJ, Cardenas-Blanco A, Kanowski M, Jessen F, Duzel E. In vivo MRI assessment of the human locus coeruleus along its rostrocaudal extent in young and older adults. Neuroimage 2017;163:150–9.
[46] Acosta-Cabronero J, Betts MJ, Cardenas-Blanco A, Yang S, Nestor PJ. Vivo MRI Mapping of Brain Iron Deposition across the Adult Lifespan. J Neurosci 2016;36:364–74.
[47] Acosta-Cabronero J, Williams GB, Cardenas-Blanco A, Arnold RJ, Lupson V, Nestor PJ. In vivo quantitative susceptibility mapping (QSM) in Alzheimer's disease. PLoS One 2013;8:e81093.
[48] van Bergen JMG, Li X, Quevenco FC, Gietl AF, Treyer V, Meyer R, et al. Simultaneous quantitative susceptibility mapping and Flutemetamol-PET suggests local correlation of iron and beta-amyloid as an indicator of cognitive performance at high age. Neuroimage 2018;174:308–16.
[49] Ayton S, Fazlollahi A, Bourgeat P, Raniga P, Ng A, Lim YY, et al. Cerebral quantitative susceptibility mapping predicts amyloid-beta-related cognitive decline. Brain 2017;140:2112–9.
[50] Acosta-Cabronero J, Cardenas-Blanco A, Betts MJ, Butryn M, Valdes-Herrera JP, Galazky I, et al. The whole-brain pattern of magnetic susceptibility perturbations in Parkinson's disease. Brain 2017; 140:118–31.
[51] Kim EY, Sung YH, Shin HG, Noh Y, Nam Y, Lee J. Diagnosis of Early-Stage Idiopathic Parkinson's Disease Using High-Resolution Quantitative Susceptibility Mapping Combined with Histogram Analysis in the Substantia Nigra at 3 T. J Clin Neurol 2018;14:90–7.
[52] Langkammer C, Pirpamer L, Seiler S, Deistung A, Schweser F, Franthal S, et al. Quantitative Susceptibility Mapping in Parkinson's Disease. PLoS One 2016;11:e0162460.
[53] Dusek P, Skoloudik D, Maskova J, Huelnhagen T, Bruha R, Zahorakova D, et al. Brain iron accumulation in Wilson's disease: A longitudinal imaging case study during anticopper treatment using 7.0T MRI and transcranial sonography. J Magn Reson Imaging 2018;47:282–5.
[54] Acosta-Cabronero J, Machts J, Schreiber S, Abdulla S, Kollewe K, Petri S, et al. Quantitative Susceptibility MRI to Detect Brain Iron in Amyotrophic Lateral Sclerosis. Radiology 2018; 289:195–203.
[55] Costagli M, Donatelli G, Biagi L, Caldarazzo Ienco E, Siciliano G, Tosetti M, et al. Magnetic susceptibility in the deep layers of the primary motor cortex in Amyotrophic Lateral Sclerosis. Neuroimage Clin 2016;12:965–9.
[56] Meineke J, Wenzel F, De Marco M, Venneri A, Blackburn DJ, Teh K, et al. Motion artifacts in standard clinical setting obscure disease-specific differences in quantitative susceptibility mapping. Phys Med Biol 2018;63:14NT01.
[57] Zhang N, Song X, Bartha R, Beyea S, D'Arcy R, Zhang Y, et al. Advances in high-field magnetic resonance spectroscopy in Alzheimer's disease. Curr Alzheimer Res 2014;11:367–88.
[58] Zaiss M, Bachert P. Chemical exchange saturation transfer (CEST) and MR Z-spectroscopy in vivo: a review of theoretical approaches and methods. Phys Med Biol 2013;58:R221–69.
[59] Waragai M, Moriya M, Nojo T. Decreased N-acetyl aspartate/Myo-Inositol ratio in the posterior cingulate cortex shown by magnetic resonance spectroscopy may be one of the risk markers of preclinical Alzheimer's disease: A 7-year follow-up study. J Alzheimers Dis 2017; 60:1411–27.
[60] van de Bank BL, Emir UE, Boer VO, van Asten JJ, Maas MC, Wijnen JP, et al. Multi-center reproducibility of neurochemical profiles in the human brain at 7 T. NMR Biomed 2015;28:306–16.
[61] Voelker MN, Kraff O, Brenner D, Wollrab A, Weinberger O, Berger MC, et al. The traveling heads: multicenter brain imaging at 7 Tesla. MAGMA 2016;29:399–415.
[62] (GUFI). GUFI. Approval of subjects for measurements at ultra-high-field MRI. https://mr-gufi.de/images/documents/Approval_of_subjects_for_measurements_at_UHF.pdf. Accessed June 11, 2019.
[63] Clarke W, Mougin O, Driver I, Rua C, Carpenter A, Muir K, et al. The UK7T Network – optimized design of a multi-site, multi-vendor travelling heads study. Proc 26th Meet Int Soc Magn Reson Med 2018.